Distinct SIV-Specific Lymphoid Tissue CD8 T cells Simultaneously Exhibit Effector and Stem-like Profiles and Associate with Viral Control and Reduced Reservoir Size

329

Zachary Strongin[1], Claire Deleage[2], Timothy N. Hoang[1], Laurence Raymond Marchand[1], Gregory K. Tharp[1], Kevin Nguyen[1], Andrew R. Rahmberg[3], Jason M. Brenchley[3], Steven E. Bosinger[1], Haydn T. Kissick[1], Mirko Paiardini[1]

[1]Emory University, Atlanta, GA, USA, [2]Frederick National Laboratory for Cancer Research, Frederick, Maryland, USA, [3]Laboratory of Viral Diseases, NIAID, NIH, Bethesda MD, USA

INTRODUCTION

HIV cure efforts are increasingly focused on strategies targeting CD8 T cell functionality, particularly in lymphoid tissues where the viral burden is high, and CD8 T cells exhibit a unique profile. Thus, a better understanding of the features of CD8 T cells promoting HIV control can critically inform therapeutic design. Work in other chronic diseases has recently revealed critical roles for the transcription factor TOX, a driver of the CD8 exhaustion program, and TCF1, the main regulator of stem-like CD8 T cells that feeds the effector pool and provides responsiveness to immunotherapies.

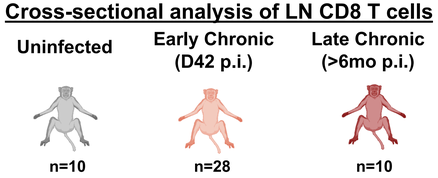
AIMS

- Investigate the dynamics of TOX and TCF1-expressing CD8 T cells in lymph nodes (LN) during SIV infection
- Evaluate the relationship between LN CD8 T cell populations and viral burden in early chronic SIV infection

RESEARCH DESIGN

We evaluated the phenotypic (flow cytometry), functional (SIV peptide stimulations) and transcriptional (single-cell RNA-seq) profiles in addition to the localization (immunofluorescence imaging) of lymph node CD8 T cells during SIV infection.

Cross-sectional analysis of LN CD8 T cells



RESULTS

TOX is highly expressed on CD8 T cells after infection and is co-expressed with inhibitory receptors

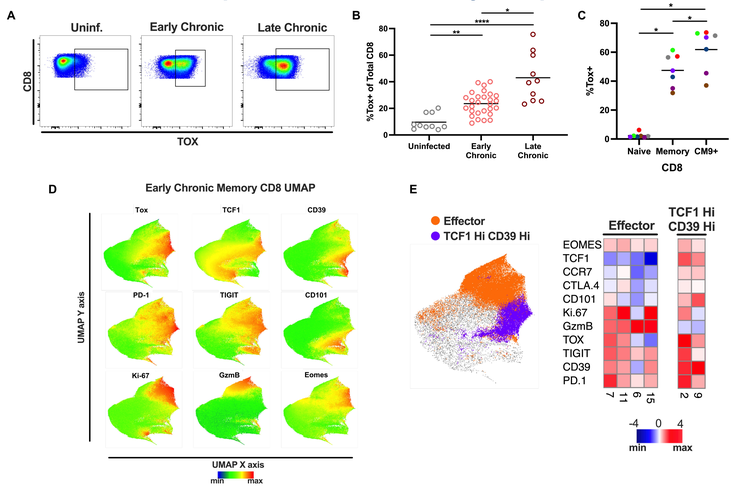


Figure 1. TOX expression and CD8 phenotype during SIV infection. A) Representative staining of TOX in LN total CD8 T cells in RMs at various infection stages. B) TOX expression in LN total CD8 T cells in uninfected RMs (n=10), during early chronic infection (n=28; D42 p.i.) and late chronic infection (n=10; >6 months p.i.). C) TOX expression within LN CD8 T cell subsets of A*01+ RMs (n=7) at early chronic infection. D) UMAP plot of flow cytometry data showing expression patterns of markers of interest. E) Heatmap of expression measured of markers of interest within a subset of clusters identified through Phenograph analysis of flow cytometry data that represent traditional effector cells and TCF1 Hi CD39 Hi cell clusters. P values determined using Kruskal-Wallis one way-ANOVA with Dunn's multiple comparisons. *$P < 0.05$, **$P < 0.01$, ***$P < 0.001$, ****$P < 0.0001$.

TCF1⁺ CD39⁺ CD8 T cells expand in LN after SIV infection and display a unique phenotypic profile

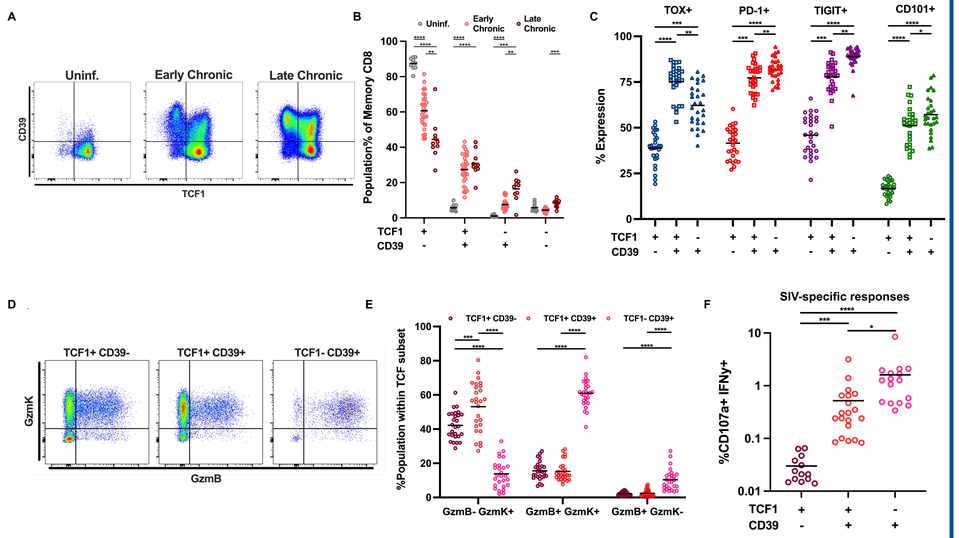


Figure 2. TCF1⁺ CD39⁺ CD8 T cells expand after SIV infection and are a unique phenotypic population. A-B) Representative staining of TCF1 and CD39 and (B) proportion of LN memory CD8 T cells falling within TCF1/CD39 subsets in uninfected RMs (n=10), during early chronic infection (n=28; D42 p.i.) and late chronic infection (n=10; >6 months p.i.). C) Expression of traditional inhibitory markers within TCF1/CD39 subsets of LN memory CD8 during early chronic infection (n=28). D) Representative staining of granzyme B and granzyme K and (E) proportion of cells within each TCF1/CD39 subset expressing one or both of GzmB and GzmK within LN memory CD8 T cells during early chronic infection (n=28). F) Proportion of cells within each TCF1/CD39 subset expressing CD107a in combination with production of IFNγ after 6hr ex vivo stimulation of LN cells with SIV GAG peptide pool. Only animals exhibiting significant responses (>0.01% of cells responding) are shown. P values determined using two-way ANOVA with Tukey's multiple comparisons test (B) and Kruskal-Wallis one way-ANOVA with Dunn's multiple comparisons (C-F). *$P < 0.05$, **$P < 0.01$, ***$P < 0.001$, ****$P < 0.0001$.

Transcriptional profiling of SIV-specific LN CD8 reveals intermediate effector cell population maintaining stem-like properties

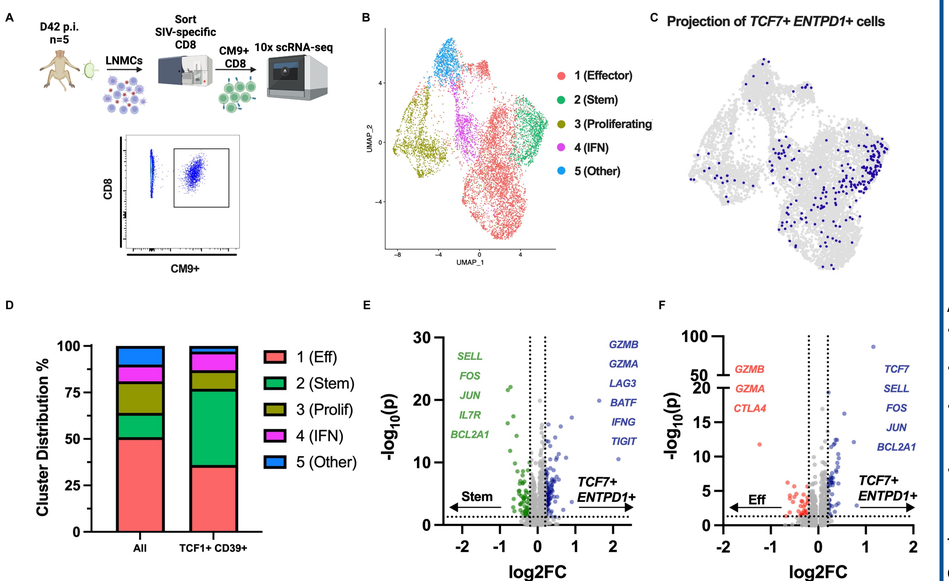


Figure 3. scRNA-seq of SIV-specific LN CD8 reveals distinct transcriptional clusters A) Study schematic depicting sorting of SIV-specific CD8 T cells (D42 p.i.) and downstream scRNA-seq. Representative stain of SIV-specific cells is shown. B) UMAP analyses of SIV-specific LN CD8 T cells from 5 RMs at early chronic infection were combined to identify 5 distinct clusters. C) Projection of cells expressing both *TCF7* and *ENTPD1* onto UMAP plot. D) Distribution of all SIV-specific cells and *TCF7+ ENTPD1+* cells across the 5 identified clusters. E-F) Violin plot displaying differentially expressed genes between E) Stem (2) cluster and *TCF7+ ENTPD1+* cells and F) Effector (1) cluster and *TCF7+ ENTPD1+* cells. Selected genes with significantly different expression are listed.

TOX⁺ and TCF1⁺ CD39⁺ CD8 T cells are strongly associated with viral control

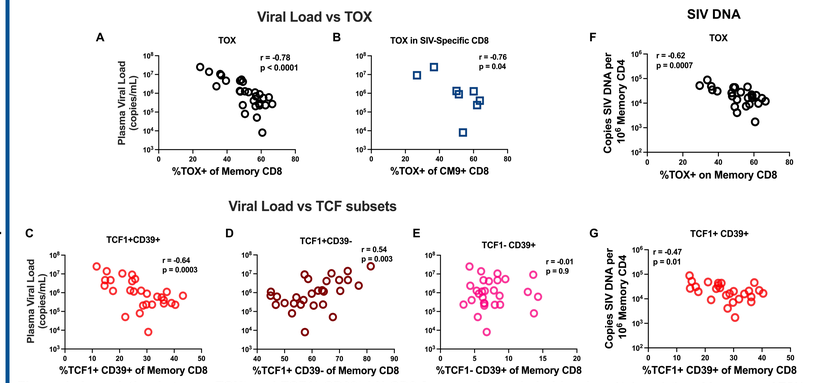


Figure 4. Association between TOX⁺ and TCF1⁺ CD39⁺ LN CD8 frequencies and viral burden. A) Association of frequency of TOX+ cells within LN memory CD8 and plasma viral load (n=28). B) Association between expression of TOX by SIV-specific LN CD8 and plasma viral load (n=8). C-E) Association of frequency of TCF1/CD39 subsets within LN memory CD8 and plasma viral load (n=28). F-G) Association of frequency of f) TOX+ or g) TCF1+ CD39+ cells within LN memory CD8 and total SIV DNA within LN memory CD4 (n=26).

TOX+ and TCF1⁺ CD39⁺ CD8 T cells express CXCR5 and are found at increased frequency within B cell follicles

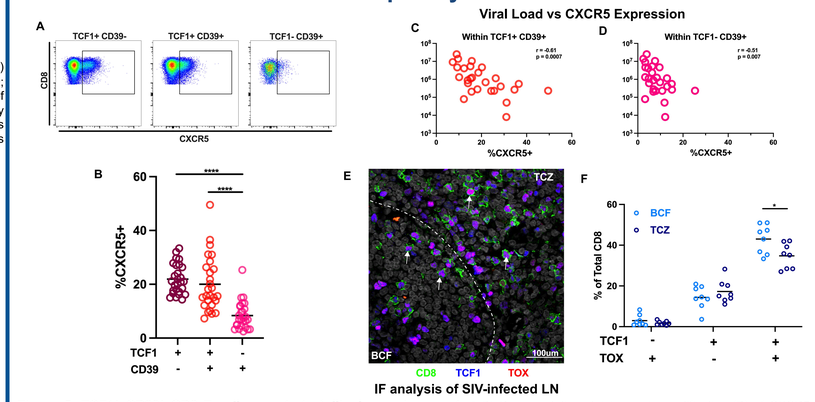


Figure 5. TCF1⁺ CD39⁺ CD8 T cells penetrate follicular environment. A-B) Representative staining and quantification (B) of CXCR5 expression within TCF1/CD39 memory CD8 T cell subsets in LN during early chronic infection (n=27; D42 p.i.). C-D) Association of CXCR5 expression within TCF1/CD39 subsets and plasma viral load (n=27; D42 p.i.). I) Representative image of immunofluorescence analysis identifying TCF1+ and TOX+ CD8 T cells in LN. Arrows designate examples of TCF1+ TOX+ CD8+ cells. J) Quantification of proportion of CD8 T cells expressing TOX and TCF1 within B cell follicles and T cell zone (n=8; D42 p.i.). Differences in CXCR5 expression were determined using Kruskal-Wallis one way-ANOVA with Dunn's multiple comparisons. Correlations were determined using Spearman analysis. Differences in BCF and TCZ CD8 populations were determined by 2-way ANOVA with Sidaks multiple comparison test. *$P < 0.05$, ****$P < 0.0001$.

CONCLUSIONS

A unique subset of TCF1⁺CD39⁺ CD8 expands in LN after SIV infection that are:

- High in TOX and inhibitory receptor expression
- Low in traditional cytotoxic molecules but high in Granzyme K
- Display phenotypic and transcriptional hallmarks of effector cells while maintaining stem-like properties
- Strongly associated with better control of plasma viremia, lower SIV DNA levels and better CD4 preservation

These cells, found at a high frequency in B cell follicles, possess both stem-like and effector features and could potentially serve as a target in future therapeutic interventions.

Acknowledgements

We would like to thank the veterinary and animal care staff at ENPRC. Drugs for the ART regimen were provided by Merck. This work was supported by NIAID (R37AI141258), ORIP/OD (P51OD011132 and U42-OD011023 to ENPRC), and the Martin Delaney Collaboratory for HIV Cure Research NIAID/NHLBI/NIDDK/NINDS/NIDA (UM1AI164562).